Tectonophysics 691 (2016) 375–384

Contents lists available at ScienceDirect

Tectonophysics

journal homepage: www.elsevier.com/locate/tecto

New constraints shed light on strike-slip faulting beneath the southern Apennines (Italy): The 21 August 1962 *Irpinia* multiple earthquake

Paola Vannoli [a,*], Fabrizio Bernardi [a], Barbara Palombo [a], Gianfranco Vannucci [b], Rodolfo Console [a,c], Graziano Ferrari [a,b]

[a] Istituto Nazionale di Geofisica e Vulcanologia, sezione Roma 1, Via di Vigna Murata, 605, I-00143 Rome, Italy
[b] Istituto Nazionale di Geofisica e Vulcanologia, sezione di Bologna, Via Donato Creti, 12, I-40127 Bologna, Italy
[c] Centro di Geomorfologia Integrata per l'Area del Mediterraneo, Potenza, Italy

ARTICLE INFO

Article history:
Received 18 July 2016
Received in revised form 27 October 2016
Accepted 30 October 2016
Available online 1 November 2016

Keywords:
1962 *Irpinia* earthquake
Multiple earthquake
Focal mechanism
Strike-slip faulting
Active tectonics
Seismic hazard

ABSTRACT

On 21 August 1962 an earthquake sequence set off near the city of Benevento, in Italy's southern Apennines. Three earthquakes, the largest having M_w 6.1, struck virtually the same area in less than 40 min (at 18:09, 18:19 and 18:44 UTC, respectively). Several historical earthquakes hit this region, and its seismic hazard is accordingly among the highest countrywide. Although poorly understood in the past, the seismotectonics of this region can be revealed by the 1962 sequence, being the only significant earthquake in the area for which modern seismograms are available.

We determine location, magnitude, and nodal planes of the first event (18:09 UTC) of the sequence. The focal mechanism exhibits dominant strike-slip rupture along a north-dipping, E-W striking plane or along a west-dipping, N-S striking plane. Either of these solutions is significantly different from the kinematics of the typical large earthquakes occurring along the crest of the Southern Apennines, such as the 23 November 1980 *Irpinia* earthquake (M_w 6.9), caused by predominant normal faulting along NW-SE-striking planes.

The epicentre of the 21 August 1962, 18:09 event is located immediately east of the chain axis, near one of the three north-dipping, E-W striking oblique-slip sources thought to have caused one of the three main events of the December 1456 sequence (I_o XI MCS), the most destructive events in the southern Apennines known to date. We maintain that the 21 August 1962, 18:09 earthquake occurred along the E-W striking fault system responsible for the southernmost event of the 1456 sequence and for two smaller but instrumentally documented events that occurred on 6 May 1971 (M_w 5.0) and 27 September 2012 (M_w 4.6), further suggesting that normal faulting is not the dominant tectonic style in this portion of the Italian peninsula.

1. Introduction

On 21 August 1962 at 15:56 (UTC) an earthquake sequence commenced approximately 20 km east of the city of Benevento, in the southern Apennines (southern Italy). Three larger shocks occurred within a 35 min timespan at 18:09, 18:19 and 18:44 (UTC). According to Guidoboni et al. (2007), the second shock was the most destructive event (I_o IX MCS, M_w 6.1).

Seismic hazard in the Benevento region is particularly high (Gruppo di Lavoro ZS9, 2004). Over its history, the city was repeatedly struck by earthquakes that produced many causalities and severe damage (Figs. 1 and 2). Notable earthquakes occurred in 1456 (M_w 6.9), 1688 (M_w 7.0), 1702 (M_w 6.5), 1732 (M_w 6.6), 1930 (M_w 6.6) (Guidoboni et al., 2007; Rovida et al., 2011), and lower magnitude sequences occurred in 1990–1992, 1997–1998, 2012, and 2016, to mention just the most recent ones (Milano et al., 2006; ISIDe Working Group, 2016).

The largest historical and instrumental earthquakes of the region occurred within a relatively narrow corridor along the axis of the Apennines chain (panel A in Fig. 1; Guidoboni et al., 2007; Rovida et al., 2011). The moment tensor solutions of the largest recent events show that the axial zone of the chain is characterized by normal faulting with NE-SW oriented T axes (see panels B and C in Fig. 1). The southern Apennines would therefore appear to be dominated by extension perpendicular to the NW-SE trend of the chain, with a strike-slip regime dominant in the Gargano Promontory (panels B and C in Fig. 1). Normal faulting regime should include the Benevento region, where no damaging earthquakes have been instrumentally recorded so far Fig. 1 and references therein), although the focal mechanisms available for the area do show some complexity (panels B and C in Fig. 1).

The 21 August 1962 earthquakes are thus key events to understand the seismotectonic setting of this stretch of the Apennines. The epicentral area of the 1962 sequence is located near Benevento, between the

* Corresponding author.
E-mail address: paola.vannoli@ingv.it (P. Vannoli).

http://dx.doi.org/10.1016/j.tecto.2016.10.032
0040-1951/

well-known NW-SE striking normal faults of the Apennines chain axis and a roughly E-W striking, oblique-to-strike-slip fault system that was postulated based on regional subsurface geology and historical seismicity (Fig. 2; DISS Working Group, 2015 and reference therein).

Previous instrumental analyses of this sequence were poorly constrained due to the incompleteness of the instrumental datasets available to these early workers. In particular, the seismogenic sources responsible for the three main events of the 21 August 1962 sequence are largely unknown. Despite the 1962 events being relatively recent, no attempt has been made to attribute these earthquakes to specific faults, in part due to the inherent difficulties in the investigation of a sequence of earthquakes of comparable magnitude that are tightly clustered in time and space. Complex earthquake sequences are rather common over the whole Italian territory, may have any kinematics (see Table 4 in Vannoli et al., 2015a), and their investigation is especially challenging. The identification of the faults responsible for the largest shocks of the 1962 sequence is made even harder by (a) the lack of reported surface faulting, (b) the geological complexity of the area, and (c) the absence of reliable focal mechanisms.

Standard analyses that treat the spatial distribution of macroseismic intensities (e.g. the Boxer code by Gasperini et al., 1999, 2010) have been extensively and successfully used to support the characterization of many Apennines earthquakes (e.g. Vannoli et al., 2015b). However, these are of little use when dealing with complex sequences where the damage areas of adjacent and quasi-contemporaneous multiple earthquakes of comparable magnitude coalesce, thus making respective effects indiscernible. We maintain that a detailed elaboration of the available instrumental data and a geological perspective upon the results are the only means to identify the seismogenic sources of such multiple earthquakes.

Earthquakes focal mechanisms are among the most valuable data to assess the geometric and kinematics parameters of seismogenic faults, along with location and magnitude estimates. Vannoli et al. (2015b) recently derived the main source parameters of the M_w 5.8, 30 October 1930 Senigallia, central Italy earthquake by retrieving, processing and analyzing a large number of historical seismograms collected, digitized, and stored by SISMOS (http://sismos.ingv.it) for that event – and for many more. These seismograms represent an invaluable source of information for the seismotectonics analysis of key earthquakes of the 20th century.

Building on that experience, in this paper we carried out a comprehensive review of the 1962 sequence in search of its causative faults, with a detailed instrumental analysis of the first event. We calculated new seismic parameters, including earthquake location, seismic moment, magnitude estimate, and focal mechanism.

The occurrence of three relatively strong shocks in close space and time proximity caused the contamination of individual event signals (see in Fig. 1 in supplementary information), so that estimating the focal mechanism of the first mainshock with the method applied in Vannoli et al. (2015b) and described in Bernardi et al. (2016) would return inaccurate results. Therefore, we calculated the focal mechanism solution of the 18:09 shock with the first motion polarities recorded at several European and worldwide stations.

2. Seismotectonic settings

The Southern Apennines chain is an east-verging fold-and-thrust belt related to the west-dipping subduction of the Apulian lithosphere (e.g. Doglioni et al., 1996). Both the Apennines subduction and the related accretionary wedge and back-arc extension migrated eastward, incorporating sediments deposited over the Mesozoic passive continental margin of the Adriatic plate and of the Ionian oceanic

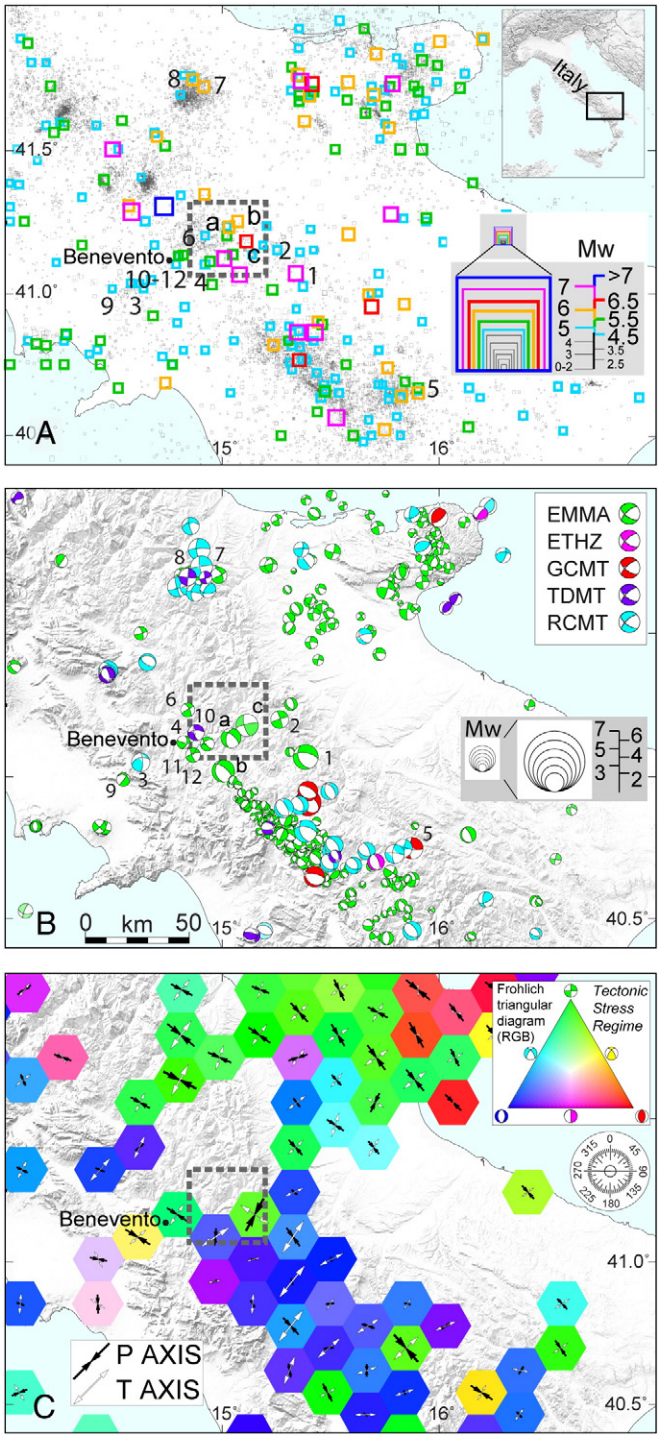

Fig. 1. Panel A: Instrumental and historical earthquakes with (original or proxies) magnitude M_w in Italy (Gasperini et al., 2013) which covers the period span from 1981 to 2014 and extended backward in time up to 1960 (unpublished report) by adding the open file CAING of the then Istituto Nazionale Geofisica. The catalogue is then extended backward in time up to 1005 adding earthquakes of CPTI (Rovida et al., 2011). Panel B: Available focal mechanisms from (a) EMMA database (Vannucci and Gasperini, 2004, and unpublished update); (b) Swiss Federal Institute of Technology in Zurich (ETHZ); (c) Global CMT Catalog (GCMT); (d) INGV-Time Domain Moment Tensor (TDMT); (e) INGV-Regional Centroid Moment Tensor (RCMT). Panel C: Focal mechanism sum, by using Kostrov (1974) technique and hexagonal mesh with a 10 km side. For each cell the tectonic style is represented with an RGB colour taken by the point of the Frohlich (1992) ternary diagram, where the corresponding focal mechanism sum is plot. P and T axes on horizontal planes are displayed. Dashed rectangle in all the panels shows the area of Fig. 4. Earthquakes of 23 July 1930 (1), 6 May 1971 (2), 14 February 1981 (3), 3 May 1990 (4), 5 May 1990 (5), 18 March 1992 (6), 31 October 2002 (7), 1 November 2002 (8), 21 May 2005 (9), 27 September 2012 (10–12, at 1:08, 3:47 and 8:35 UTC, respectively) and the sequence of 21 August 1962 (a, b, c, at: 18:09, 18:19, 18:44 UTC, respectively) are indicated in A and B panels.

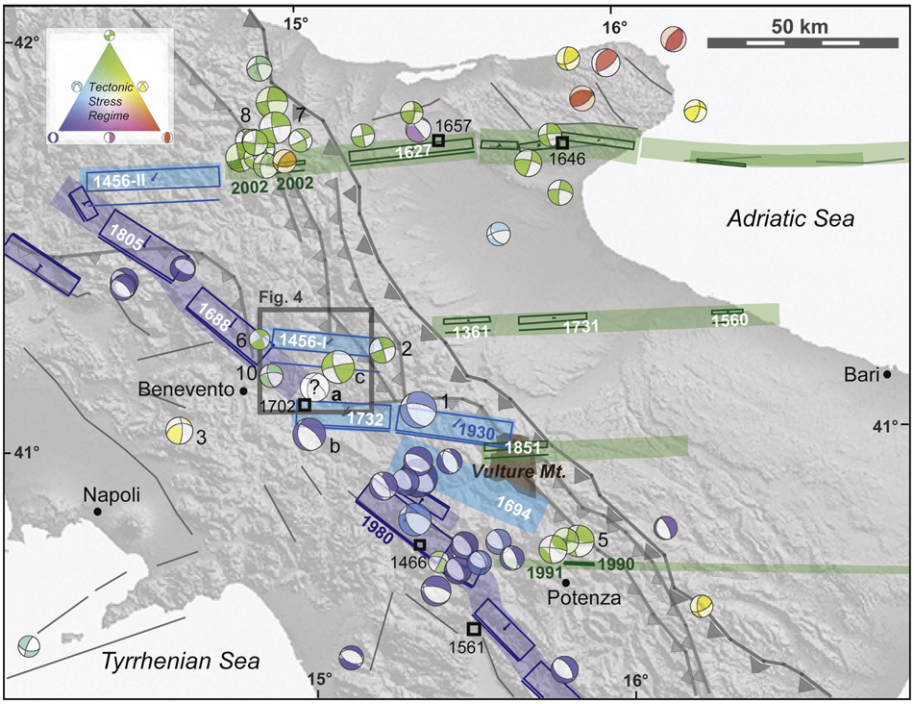

Fig. 2. Seismotectonic sketch map of the Sannio-Irpinia area and surroundings. *Individual* and *Composite seismogenic sources* are shown as rectangles and ribbons, respectively (DISS Working Group, 2015). The sources are shown with the colors of the Frohlich diagram (top right) according to their kinematics. The sources are considered responsible for the shown earthquakes (white labels refer to the sources not supported by a focal mechanism, i.e. for earthquakes occurred before the instrumental era). The focal mechanisms of earthquakes having M ≥ 4.0 are shown according to the Frohlich diagram (see Fig. 1 for the IDs of the selected events). Historical earthquakes without a seismogenic source and/or a focal mechanism are shown with black squares (Guidoboni et al., 2007). The external thrust and the main tectonic features of the southern Apennines are shown in grey (Bigi et al., 1989). Notice 1) the lack of normal focal mechanisms along the backbone of the chain in the Benevento area (with the exception of the poorly constrained focal mechanism of the second main shock of 1962 sequence); and 2) the lack of extensional sources between those responsible for the 1688 (north) and the 1980 earthquakes (south).

basin during the eastward roll-back of the subduction hinge (Malinverno and Ryan, 1986). The roll-back at the front of the Southern Apennines appears to have slowed down during the Late Pleistocene due to the interference with the thick continental Apulian swell (see Doglioni et al., 1996 and references therein). The Southern Apennines chain has been subsequently uplifted and partially dropped by large normal faults straddling its crest. In fact, the recent evolution of the chain axis has been dominated by and extension orthogonal to the NW-trending mountain belt. The Apennines have been the locus of several destructive earthquakes with magnitude up to M 7 occurring in the uppermost 12–15 km of the crust (e.g. the 23 November 1980, M_w 6.9; Fig. 2). Much of this seismicity is due to a well-documented normal faulting mechanism that can produce surface faulting, such as for the 23 November 1980 *Irpinia* (e.g. Westaway and Jackson, 1984), and the 13 January 1915 *Fucino* earthquakes (e.g. Michetti et al., 1996).

Large historical (e.g. December 1456, M_w 6.9; Guidoboni et al., 2007) and recent instrumentally-recorded (5 May 1990, M_w 5.8; 31 October 2002, M_w 5.7; 1 November 2002, M_w 5.7; Rovida et al., 2011) earthquakes have occurred in the Adriatic foreland, east of the southern Apennines chain (Fig. 2). The focal mechanisms of the 1990 and 2002 events are similar and show deep-seated strike-slip ruptures along E-W striking planes (Fig. 2).

An earthquake having M_w 6.6 (I_o XI MCS; Locati et al., 2011) took place on 23 July 1930 in the eastern portion of the Sannio-Irpinia region, WNW of the Vulture Mt. (Fig. 2). Detailed instrumental analyses suggest that 1930 earthquake ruptured a WNW-ESE plane with a dip-slip mechanism having a significant right-lateral component (Pino et al., 2008; ID 1 in Figs. 1 and 2).

The 5–30 December 1456 seismic sequence is the largest destructive sequence to have ever occurred in the southern Apennines, and is one of the strongest sequence of the entire Italian seismic history. The exceptionally large size of its damage area, its magnitude and its intensity distribution cumulates the effects of multiple shocks. On the grounds of (a) the time-and-space analysis of the earthquake sub-events, (b) the damage scenario, unfit for NW-SE trending dip-slip causative sources, (c) instrumental evidence from adjoining strong earthquakes nearby, and (d) the presence of deep-seated regional structures ca. E-W striking, Fracassi and Valensise (2007) suggested that the 1456 multiple subevents were generated by oblique right-lateral reactivation of segments of large, pre-existing E-W fault systems (Fig. 2; DISS Working Group, 2015).

Some instrumentally recorded seismic events occurred near Benevento in the Sannio-Irpinia area (Figs. 1 and 2), and were all characterized by a more or less prevalent strike-slip component along ca. E-W striking faults: (a) the 6 May 1971 *Monteleone*, M_w 5.0 (ID 2 in Figs. 1 and 2; Gasparini et al., 1982); (b) the 14 February 1981 *Baiano*, M_w 4.9 (ID 3; Locati et al., 2011); (c) the 3 May 1990, M_w 3.9 (ID 4; Frepoli and Amato, 2000); (d) the 18 March 1992, M_w 4.1 (ID 6; Frepoli and Amato, 2000); (e) the 21 May 2005 *Irpinia*, M_w 3.5 (ID 9; Li et al., 2007); and (f) the recent 27 September 2012 *Benevento*, M_w 4.6 earthquakes (ID 10; Adinolfi et al., 2015).

All these historical and instrumental seismic events unveiled the presence of a fault system not fully understood up to now, that should involve large segments of deep-seated, E-W strike-slip to oblique-slip faults, with no (known) surface faulting. Several studies (DISS Working Group, 2015 and reference therein) suggest that such faulting belongs to inherited, pre-existing, shear zones with a long tectonic history, currently undergoing their most recent phase of right-lateral reactivation.

3. Instrumental analysis

To study the first mainshock of the 21 August 1962 sequence we used records from the database of the INGV - SISMOS project. The SISMOS project, initiated in 2001 by Istituto Nazionale di Geofisica e Vulcanologia (INGV) scientists, involves digitizing, archiving and

distributing historical seismograms, station bulletins, log books, and related information retrieved from Italian and Euro-Mediterranean observatories, with data from as far back as 1895 (Michelini et al., 2005; Ferrari and Pino, 2003; http://sismos.ingv.it). So far, SISMOS has retrieved and processed seismograms recorded by about a thousand strong earthquakes occurred in the Euro-Mediterranean area since the late 19th century.

The 1962 seismic sequence occurred in a peculiar period of the history of instrumental seismology. The early 1960s are considered a turning point in modern seismology, having witnessed the rise of two standardized global networks: the *World-Wide Standardized Seismograph Network* (WWSSN) by USA initiative (Peterson and Hutt, 2014), and the *Unified Seismic Observation System* (ESSN) by the former USSR (Shishkevish, 1974). Both networks were officially installed for global seismology purposes, although both USA and USSR were interested in the detection of underground nuclear explosions. In any case, the time was ripe for modern seismology to get hold of accurately calibrated and accurately timed standardized seismographs.

The installation of WWSSN stations started in October 1961 and was completed in 1967. Out of 127 stations, 54 were installed before the 1962 earthquakes, only 11 of which in the Euro-Mediterranean area. The ESSN consisted of 168 seismic stations, either already existing or new ones. Short-period and long-period Kirnos system seismographs (e.g. SKD, SK, SKM, Vegik) were the most widely used in the ESSN. China, France, French-speaking countries in Africa, and Canada did not participate in either network.

As regards seismology, the development of these networks meant that, for the first time, the variation of waveform amplitude, shape, and timing could be compared over a broad region - or the entire Earth - to infer characteristics of the source and propagation medium using quantitative seismology (Peterson and Hutt, 2014).

However, most of the Euro-Mediterranean seismological observatories and stations continued to operate with the most diverse and heterogeneous instrumentation, often designed at the beginning of the 20th century. In particular, these consisted of mechanical seismographs, such as Wiechert and Mainka, or electromagnetic ones with galvanometric recording, such as Galitzin.

The use of seismograms recorded by the latter instruments is constrained by difficulties arising from (1) static magnification, which in general is significantly smaller than WWSSN seismographs or modern digital broadband seismometers, causing smaller amplitudes and less waveform details; (2) the irregular speed of the seismograph's drum, which introduces phase distortions in the seismograms; (3) fast motion of the seismograph recording system (nib for mechanical seismographs, light beam for galvanometric ones) that causes weak or absent traces on the recordings of stations close to the epicenter; (4) the inaccurate synchronization of the station clock used for reading arrival times; (5) the limited frequency range response and short periods of seismographs (1–20 s and 10–30 s for mechanical and electromagnetic instruments, respectively; Bernardi et al., 2005); and (6) uncertain knowledge of the polarity of the seismographs (direction of motion of the steady mass corresponding to upward motion on the seismogram).

For the 21 August 1962 earthquakes, the SISMOS database supplied 245 high-resolution scans (300 components) of the seismograms recorded at 58 different stations by 40 different standard and non-standard instruments, both on smoked and photographic paper. The magnification for the different types of seismographs ranges from 60 to 300 (30%) for mechanical recording, from 1000 to 3000 (Long Period - LP - , 40%), and from 20,000 to 100,000 (Short Period - SP - , 10%) for galvanometric recording.

To calculate the focal mechanism of the first main shock (18:09 UTC) we analyzed the available 300 records; despite such large number, it was possible to unambiguously recognize just 29 polarities. This is due mainly to: (a) background noise that “covers” frequently weak amplitudes of first motions; (b) low amplification of the mechanical instruments; (c) the distance of many long period seismographs; and (d) the first motion corresponding to the time-mark, often represented by an interruption of the track.

In addition, one of the many critical issues in the use of historical seismograms is the knowledge of the polarity of the seismographs with mechanical and galvanometric recording system that operated in the Euro-Mediterranean area. This information is not easy to find and rarely appears in the seismological literature or seismic bulletins. Periodical collections, on a global scale, of these and other information of instrumental parameters are not always reliable or they do not refer to the same convention of polarity.

Therefore, when not indicated on the seismogram, one needs to search for the instrumental polarity in the available literature, paying attention to the convention used by the source of information. One of these important sources for such data is Charlier and Van Gils (1953), which, however, uses a convention different from that in use since the introduction of WWSSN. In particular, the authors consider an upward movement in the seismogram (+): the movement of the mass downward, in the direction E and in the direction N. According to the convention in use, only the polarity of the vertical component indicated by Charlier and Van Gils (1953) is coincident, while it is the opposite for the horizontal components.

3.1. Location

A list of hypocentral coordinates for the 21 August 1962, 18:09 earthquake available in literature is reported in Table 1. The first instrumental location was published by Di Filippo and Peronaci (1963). As remarked by Westaway (1987), their results were unreliable due to the poor azimuthal distribution of the few regional stations used in the location algorithm, covering mainly the NW quadrant, except for one station to the SE (Ksara). A more robust location, based on a much larger number of stations, was reported in the ISS bulletin (1967). In the following years, the hypocentral coordinates were published in other papers such as Carrozzo et al. (1973), and Westaway (1987). Finally, this earthquake was also included in the ISC-GEM Global Instrumental Earthquake Catalogue (Storchak et al., 2013), as the result of a special effort to improve currently existing bulletin data of large global earthquakes by means of modern location algorithms and Earth models.

Westaway (1987) remarked that not only the first location given by Di Filippo and Peronaci (1963), but also those reported by the International Seismological Summary (ISS) are most likely biased by the uneven distribution of stations. According to his study, such locations are systematically mislocated to the north of the true epicentral area. In order to avoid or at least reduce this problem, Westaway (1987) applied a relative location technique of the 21 August 1962, 18:09 earthquake with the epicenter of the 18:19 mainshock (i.e. the highest magnitude among the 1962 events). This worker included in his calculations the epicenter of the 1980 *Irpinia* earthquake too, considered more reliably located because of the improved quality of the international seismological networks in the meantime. Unlike most of the previous studies, which locate the hypocentral depth of the 1962 earthquakes below 25 km, Westaway (1987) obtained a depth of only 8 km, based on waveform analysis.

To locate the 21 August 1962 18:09 earthquake and estimate the associated 90% confidence ellipse, we used the fully nonlinear earthquake location package NonLinLoc (NLL; Lomax, 2005) with an Equal-Differential Time (EDT) misfit function. We used data from the ISS bulletin, compared and integrated with data from station bulletins (all data available at http://sismos.ingv.it/en/index.php/bulletins) and literature (e.g. Di Filippo and Peronaci, 1963).

The NLL code performs a probabilistic hypocentral location, quantified by a Probability Density Function (PDF) in a 3D space. The PDF is obtained by means of an EDT formulation of the likelihood function, containing the calculated and observed differences between two stations, summed over all observations pairs. We adopted the ak135

Table 1
Locations, Magnitude and focal mechanisms of the first event (18:09 UTC) of the 1962 sequence from the literature. References in column "R" (1: Di Filippo and Peronaci, 1963; 2: Costantinescu et al., 1966; 3: ISS, 1967; 4: Carrozzo et al., 1973; 5: Gasparini et al., 1982, 1985; 6: Bonasia et al., 1986; 7: Westaway, 1987; 8: Kiratzi and Papazachos, 1995; 9: Storchak et al., 2013 (ISC-GEM); 10: Villaseñor and Engdahl (2005; EHB); 11: International Seismological Centre (ISC) (2015). #St: Number of stations used for the location; w: M_w; s: M_s; F: Fixed; R(n): original value taken from authors indicated by the number in column R; —: not available data.

R	Lat (°)	Lon (°)	Dep (km)	#St	M	Mo (dy ∗ cm) E24	Strike 1 (°)	Dip 1 (°)	Rake 1 (°)	Strike 2 (°)	Dip 2 (°)	Rake 2 (°)	Beach ball
1	41.171	15.116	49.5	13	–	–	83	75	–	7	58.5	–	
2	41.2	15.1	–	40	5.75	5.3	317	58	−35	67	59	−144	
3	41.23	15.01	25	177	–	–	–	–	–	–	–	–	–
4	41.1	15.1	36	–	–	–	–	–	–	–	–	–	–
5	(*R3*)	(*R3*)	(*R3*)	–	5.7	4.5	298	81	155	32	65	10	
6	(*R3*)	(*R3*)	–	–	5.7 s	6.2	(R5)	(R5)	(R5)	(R5)	(R5)	(R5)	(R5)
7	41.135	15.018	8F	66	5.2w	0.8	310	65	−130	193	46	−36	
8	41.0	15.0	–	–	5.6 s	4.67							
9	41.25	15.07	20F	–	–	–	–	–	–	–	–	–	–
10	41.178	14.993	20F	169	5.6 s	–	–	–	–	–	–	–	–
11	41.248	15.070	20F	180	–	–	–	–	–	–	–	–	–

model (Kennett, 2005) for teleseismic phases, and a standard Italian crustal model (Basili et al., 1984) for local phases. The NLL procedure converges to the final solution (41.22°N, 15.01°E, and 9 km depth) after five iterations, using 44 phases (out of 352; 25 P and 19 S) from 39 stations (out of the 179 available ones), with a maximum azimuthal gap of ca. 90° (Fig. 3). Arrival phases were both automatically and manually re-associated, and the outliers were deleted at each iteration. However, the formulation of the EDT function (Lomax, 2005) is such that the method is relatively unaffected by the presence of outliers.

3.2. Magnitude

Our dataset for this event consists of both low-gain analog and long-period electromagnetic regional seismograms recorded by high gain

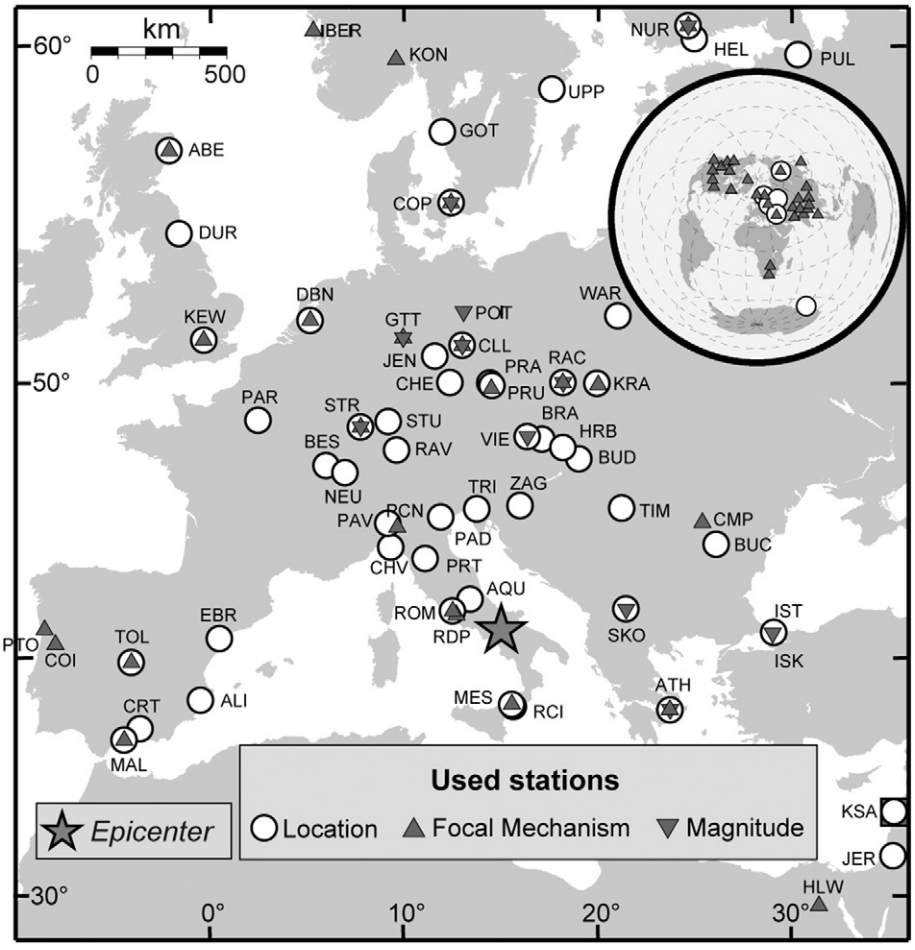

Fig. 3. Stations with seismograms used to assess epicentral location, magnitude, and focal mechanism of the first shock of the 1962 sequence.

and high quality WWSSN seismographs (Fig. 3). We thus determine earthquake size from the well recorded surface waves.

The surface wave magnitude M_S, originally defined by Gutenberg (1945) and later by Soloviev (1955), Kárník et al. (1962), and Vanëk et al. (1962), is proportional to the maximum ground velocity given by the term $(A/T)_{max}$:

$$M_S = \left(\frac{A}{T}\right)_{max} + 1.66 * \quad \log\Delta + Cp$$

where A is ground displacement in micrometers and T is the corresponding period in seconds, distance Δ is in degrees, and C_p equals 3.3 (Kárník et al., 1962). Common current practice is to measure the maximum ground displacement at a reference periods $T_{20} = 20$ s at teleseismic distance. At local and regional distances ($\Delta \leq 20°$) surface waves are dominated by shorter period signals, and $(A/T)_{max}$ is significantly larger than $(A_{max}/T20)$. Therefore, measuring A_{max} at T_{20} leads to systematic bias of M_s for smaller events that are predominantly recorded at close-by stations.

As already mentioned above, our dataset consists only of waveforms recorded at regional distance (Table 2). To avoid distance dependent M_s values, we apply the method described by Bernardi et al. (2005). Such method computes M_w from surface waves amplitudes for events recorded at regional distance.

We measure maximum surface wave amplitudes (one half of peak-to-peak values) from digitized seismograms. We correct the amplitudes to account for gain difference between true measurement period T_ω and reference period T_Δ, where

$$T_\Delta = -3.99 + 6.41 \cdot \ln(\Delta)$$

The reference period T_Δ indicates the appropriate period at which the amplitude should be measured with respect to the epicentral distance of the seismic station.

For digitized seismograms, the maximum amplitude A_ω is measured at period T_ω with gain V_ω (see Bernardi et al., 2005). At period T_Δ, the amplitude would be $A_\omega \cdot (V_\Delta/V_\omega)$ (V_Δ is the gain at T_Δ). The true ground displacement at T_Δ is then $A_\omega \cdot (V_\Delta/V_\omega) \cdot (1/V_\Delta$. The amplitude-$M_o$ relation for early instrumental earthquakes then becomes:

$$\log M_o = \log\left(\frac{A_\omega}{V_\omega}\right) - \log T_\Delta + 1.66 \cdot \log\Delta + K$$

where $K = 14.90 \pm 0.32$ is calibrated for events occurred and recorded in the Euro-Mediterranean area, and where $A\omega$ is the vector sum of the two horizontal components (Bernardi et al., 2005). For stations where only one horizontal component was available, we added 0.15 units to log M_o, which assumes that the average maximum amplitudes on both horizontal components are the same.

Table 2 shows all measured amplitudes A_x and periods T_ω for each seismograms used in this study, including the instrument constants used to compute V_ω. Responses of the electromagnetic instruments are described in Galitzin (1914), Hagiwara (1958), and Willmore (1979). Table 3 shows the M_o values obtained for each station. The average magnitude for the event is M_w 5.5 ± 0.4.

3.3. Focal mechanism

Several studies available in the literature proposed focal mechanism solutions for the earthquake of 21 August 1962 at 18:09 considered in our study (Table 1). A comprehensive review of the studies previously carried out on both the focal mechanism of this earthquake and that of the larger magnitude mainshock, occurred 10 min later, was published by Westaway (1987).

As mentioned above, the first study on the location and focal mechanism of the two earthquakes (18:09 and 18:19) of the 1962 sequence was published by Di Filippo and Peronaci (1963). For the focal mechanism determination they adopted the graphical method introduced by Byerly (1928, 1942), still popular at the time of their study, before the introduction of computational methods. Because of a misinterpretation of the Byerly's method, the solution obtained by these authors is biased by the arbitrary constraint that the strike directions of the two possible fault planes (and not the focal planes themselves) should be normal to each other. In fact, once the first circle representing the intersection of one fault plane was drawn on the stereographic anti-polar projection, Di Filippo and Peronaci (1963) used to draw the second circle by merely selecting its radius according to the observed polarities. In doing so, though, they imposed that the centre of the second circle should be located on the tangent to the first circle on the origin of the projection coordinates. This kind of solution cannot be represented by two orthogonal nodal planes, and is valid only when both planes are vertical (plain strike-slip faulting). Moreover, the focal mechanism obtained by Di Filippo and Peronaci (1963) shows only strike and dip of the two possible fault planes but lacks rake, either in value or in a plot to choose the rake from (Table 1). The correct way of applying the Byerly's method was clearly described by De Bremaecker (1956).

Table 2
Seismograms used to compute M_w. For each used seismogram the table is giving: the station code, the component (C), the type of instrument (P for mechanical, G for electromagnetic), the station coordinates, the epicentral distance (Δ), the observed amplitude (A_x) and the observed period (T_x), and the instrument parameters. For mechanical instruments the static amplification (V_o,), the free period (T_o) and the damping constant (h) are reported. For WWSSN long period seismometers (*) the maximal magnification V_{max} and all parameters are available on Peterson and Hutt (2014).

Station	C	Type	Lat (°)	Lon (°)	Δ (°)	A_x (mm)	T_x (*sec*)	Vo	To	h
ATH	N	P	37.97	23.72	7.46	1.90	7.74	80.00	5.80	0.46
CLL	E	P	51.31	13.00	10.19	8.4	14.4	150.00	10.00	0.50
CLL	N	P	51.31	13.00	10.19	4.9	12.9	150.00	10.00	0.50
GTT	E	P	51.55	9.96	10.90	12.60	13.50	1920.00	1.47	0.40
GTT	N	P	51.55	9.96	10.90	8.50	12.00	2150.00	1.39	0.40
POT	E	P	52.38	13.07	11.25	22.70	3.60	250.00	8.00	0.43
RAC	E	P	50.08	18.19	9.14	30.60	3.00	104.00	6.00	0.40
RAC	N	P	50.08	18.19	9.14	28.10	3.00	134.00	6.00	0.40
SKO	E	P	41.97	21.44	4.88	28.50	12.3	156.00	9.00	0.37
SKO	N	P	41.97	21.44	4.88	42.10	12.7	180.00	9.00	0.37
STR	E	P	48.58	7.77	8.97	11.30	3.20	145.00	8.40	0.50
STR	N	P	48.58	7.77	8.97	26.70	3.60	145.00	8.40	0.49
VIE	E	P	48.25	16.36	7.10	22.90	7.14	140.00	8.80	0.39
VIE	N	P	48.25	16.36	7.10	21.20	6.86	165.00	9.10	0.38
GTT	E	P	51.55	9.96	10.90	12.20	8.63	160.00	12.00	0.33
STR	E	P	48.58	7.77	8.97	11.40	3.60	750.00	1.80	0.50
COP*	E	G	55.69	12.43	14.58	77.50	21.0	1500.00		
COP*	N	G	55.69	12.43	14.58	40.00	15.0	1500.00		
NUR*	N	G	60.51	24.65	20.21	64.80	13.4	3000.00		
NUR*	E	G	60.51	24.65	20.21	93.00	14.8	3000.00		
IST*	E	G	41.07	29.06	10.60	51.00	12.0	750.00		

Table 3
M_w and M_o values for each station. Only horizontal components are used. $M_w = 2/3 \log M_o$ - 6.03 (Hanks and Kanamori, 1979). "#Comp" is the number of components.

Station	#Comp	M_w	M_o (N·m)
ATH	1	5.47	2.014e + 17
CLL	2	5.48	2.074e+16
GTT	2	5.88	8.359e+17
POT	1	5.07	4.930e+16
RAC	2	5.56	2.685e+17
SKO	2	6.45	5.829e+18
STR	2	5.29	1.065e+17
VIE	2	5.78	5.785e+17
GTT	1	5.27	1.011e+17
STR	1	5.44	1.818e+17
COP	2	4.94	3.233e+16
NUR	2	4.79	1.918e+16
IST	1	5.54	2.582e+17

Table 4
Seismograms used to assess the focal mechanism of the first event (18:09 UTC) of the 1962 sequence. Identifier of the station (#), Source of the first Ground motion polarity (SoG), Station international code (Station) and its latitude (Lat) and longitude (Lon), Instrument and its component (C), polarity of the first P arrival as recorded on the seismogram (SPol), instrument polarity (IPol - i.e. direction of motion of the ground corresponding to the upward motion on the seismogram), first ground motion polarity (GPol) as result of the combination of SPol and IPol, IPolS source information for IPol. D, A and T are the station-hypocenter distance, the ray azimuth at source and ray take-off at the station respectively. Finally, the Fit column indicates whether the GPol falls (y) or not (n) in the corresponding quadrant of the focal mechanism's beachball. SoG are: ASK = Annales Seismologiques de Ksara (1963), BSC = Boletin sismico provisional de Cartuja (1962), BSM = Bulletin seismologique de Montreal (1962), DSB = Duhram Seismological Bulletin, ISC = from ISC online bulletin, TS = This study, and W = Westaway (1987). IPolS are: reported by Charlier and Van Gils (1953, ChVG), standard convention assumed because of the importance of the station (ConvAss), known by the authors experience or reported on other seismograms of the same instrument (Known), and reported on the seismogram (Seism).

#	SoG	Station	Lat (°)	Lon (°)	Instrument	C	SPol	IPol	GPol	IPolS	D (°)	A (°)	T (°)	Fit
1	TS	ABE	57.167	−2.100	Milne-Shaw	E	+	−	W	ConvAss	19.4	331	43.9	y
2	ISC	ALE	82.503	−62.350					D		47.6	350	28.9	y
3	TS	APA	67.569	33.405	Kirnos	Z	+	+	C	Seism	28.2	15	352.70	n
4	ISC	ATH	37.972	23.717	(WWSSN)				D		7.4	113	58.2	y
5	ISC	BAN	51.172	−115.558					D		78.1	331	19.8	y
6	TS	BER	60.384	5.334	Willmore	N	+	+	N	ConvAss	20.1	346	273.50	y
7	ISC	BLO	39.172	−86.522					C		76.2	307	21.5	y
8	ISC	BUL	−20.143	28.613	(WWSSN)				C		62.6	166	24.3	n
9	ISC	CDU	30.660	104.011					D		69.7	67	22.6	y
10	ISC	CHA	26.833	87.167					D		59.8	79	25.5	y
11	TS	CLL	51.308	13.003	Benioff	Z	+	+	C	Seism	10.2	353	146.31	y
12	ISC	CMP	45.268	25.038					D		8.3	58	58.1	n
13	ISC	COI	40.208	−8.412					D		17.7	274	51.1	n
14	TS	COP	55.685	12.433	WWSSN	N	+	+	N	Seism	14.6	354	206.03	y
15	TS	COP	55.685	12.433	WWSSN	Z	+	+	C	Seism	14.6	354	206.03	y
16	BSC	CRT	37.190	−3.596					C		14.9	260	55.8	y
17	TS	DBN	52.102	5.177	Galitzin	E	−	+	W	ChVG	12.8	332	181.83	n
18	ISC	DBQ	42.507	−90.683					C		72.8	312	21.5	y
19	ISC	DUG	40.195	−112.813	(WWSSN)				D		85.8	323	18.1	y
20	DSB	DUR	54.768	−1.585	Wilson-Lamison				D		17.4	327	51.1	y
21	ISC	EBM	46.390	96.260					D		56.2	55	26.0	y
22	ISC	FRU	42.833	74.617					D		43.4	67	149.9	y
23	ISC	GRS	39.500	46.333					D		23.8	84	39.4	y
24	TS	GTT	51.546	9.964	Wiechert	N	+	−	N	Known	10.9	343	156.00	n
25	TS	HLW	29.858	31.342	WWSSN	N	+	+	N	Seism	17.4	125	51.1	y
26	TS	HLW	29.858	31.342	WWSSN	E	−	+	W	Seism	17.4	125	51.1	y
27	W	IST	41.046	28.996	WWSSN						10.5	86	57.9	n
28	TS	KEW	51.468	-0.313	Galitzin	Z	−	+	D	ChVG	14.7	319	55.8	y
29	ISC	KIM	−28.752	24.780					D		70.6	171	157.9	y
30	W	KON	59.649	9.598	WWSSN	Z			D	Seism	18.7	351	43.9	n
31	TS	KRA	50.056	19.940	Charina	Z	+	+	C	Seism	9.5	20	58.1	y
32	ASK	KSA	33.823	35.890					C		18.1	107	43.9	n
33	ISC	LAN	36.050	103.833					D		66.4	62	23.2	y
34	ISC	LHA	29.637	91.037	(WWSSN)				D		61.1	75	24.9	y
35	W	MAL	36.728	−4.411	WWSSN	Z			C	Seism	15.7	260	55.8	y
36	ISC	MAT	36.543	138.207	(WWSSN)				C		86.5	42	17.5	n
37	TS	MES	38.199	15.555	Wiechert 80	Z	+	−	D	Known	3.1	172	58.3	y
38	ISC	MHT	39.200	−96.581	(WWSSN)				C		78.3	313	19.8	y
39	BSM	MNT	45.503	−76.623	(Benioff)	Z			D		62.9	308	24.3	n
40	TS	MOS	55.738	37.625	Galitzin	Z	+	+	C	ConvAss	20.7	38	41.9	y
41	TS	MOS	55.738	37.625	Galitzin	Z	+	+	C	ConvAss	20.7	38	41.9	y
42	ISC	MRG	39.633	−79.954					C		68.3	304	22.6	y
43	ISC	NDI	28.683	77.217	(WWSSN)				D		51.4	83	27.8	y
44	TS	NUR	60.509	24.649	WWSSN	E	+	+	E	Seism	20.2	14	41.9	y
45	TS	NUR	60.509	24.649	WWSSN	N	+	+	N	Seism	20.2	14	41.9	y
46	TS	NUR	60.509	24.649	WWSSN	Z	+	+	C	Seism	20.2	14	41.9	y
47	TS	NUR	60.509	24.649	WWSSN	E	+	+	E	Seism	20.2	14	41.9	y
48	TS	NUR	60.509	24.649	WWSSN	N	+	+	N	Seism	20.2	14	41.9	y
49	TS	NUR	60.509	24.649	WWSSN	Z	+	+	C	Seism	20.2	14	41.9	y
50	TS	PCN	45.050	9.667	Wiechert 1T	N	−	+	S	ChVG	5.5	316	58.3	y
51	TS	PCN	45.050	9.667	Wiechert 1T	E	−	−	E	ChVG	5.5	316	58.3	y
52	ISC	PNT	49.317	−119.617					D		81.1	332	19.2	y
53	ISC	PTO	41.139	−8.602	(WWSSN)				C		17.7	278	51.1	y
54	W	QUE	30.188	66.950	WWSSN	N			D	Seism	42.9	88	30.1	y
55	TS	PRU	49.988	14.542	Wood Anderson	N	−	−	N	Seism	8.8	358	58.1	y
56	TS	RAC	50.083	18.194	SD-57	E	−	−	E	ConvAss	9.1	13	58.1	y
57	TS	RDP	41.758	13.717	Wiechert 80	Z	+	−	D	Known	1.8	288	85.5	y
58	ISC	REN	39.540	−119.813					C		89.4	327	16.9	n
59	TS	ROM	41.903	12.513	Wiechert 1 T	N	+	+	N	ChVG	2.0	291	60.1	y
60	ISC	SCH	54.817	−66.783					C		53.1	315	27.2	y
61	ISC	SHL	25.567	91.883	(WWSSN)				D		64.0	78	23.8	y
62	ISC	SIA	34.248	108.920					D		70.8	61	22.1	y
63	ISC	SOD	67.371	26.629					D		26.9	10	33.8	y
64	TS	STR	48.585	7.766	Wiechert 1T	E	−	+	W	ChVG	9.0	328	58.1	n
65	ISC	TIF	41.717	44.800					C		22.2	79	39.4	n
66	TS	TOL	39.881	−4.049	WWSSN	Z	+	+	C	Seism	14.5	271	55.8	y
67	ISC	YAK	62.031	129.681					D		64.2	28	23.8	y

Some disagreements exist between the solutions reported in two subsequent papers too. According to Gasparini et al. (1982, 1985), the mechanism of the 18:09 event was a clear example of strike-slip faulting with WNW-ESE or NE-SW striking planes. Westaway (1987) pointed out that their solution contained numerous inconsistent polarities, and was also inconsistent with most of the long period WWSSN data. Westaway (1987) also identified predominant normal faulting with a NW-SE striking plane, parallel to the trend of the Apennines, considered as the dominant feature of the seismotectonics of the region.

In this study we integrated the first motion polarity dataset read on the SISMOS seismograms with 30 polarities from the ISC online bulletin, 4 from Westaway (1987), and 4 from selected station bulletins, for a total of 67 polarities from 58 different stations (Table 4; Fig. 3). Westaway provides 7 polarities, although just 4 of them are complementary to those read on the seismograms. Our best solution for the focal mechanism was obtained using the *Esmed_glob* unpublished code, originally developed at INGV for local networks data and then modified for teleseismic P arrivals in a spherical earth model.

Esmed_glob contains specific features that make it suitable for our study, since this code accepts polarities observed on the horizontal components, which can be weighted according to the clarity of the first onset. The algorithm performs a systematic search of the optimal set of focal parameters ϕ (strike), δ (dip) and λ (rake) in steps of 10°. The search is then restricted within smaller ranges in steps of 3°, and finally in steps of 1°. The optimal solution is automatically selected among all the possible sets of focal mechanism parameters that achieve the minimum number of inconsistent polarities. This is achieved by minimizing a misfit function based on the angular distance with respect to the nodal planes, i.e. *Esmed_glob* weights P-arrival observations by their theoretical amplitudes on the focal sphere. Finally, to assess the robustness of the final solution, the code explores the range of all the three focal parameters, so as the minimum number of inconsistent polarities remains the same.

The results for the focal mechanism for the 18:09 event are 278°, 60°, −161° and 178°, 73°, −31°, for strike, dip, and rake of the two nodal planes, respectively (as shown in Table 5 and Fig. 4). It is a predominantly strike-slip mechanism, with a normal oblique component.

The reliability of our solution is supported by the good azimuth and distance distribution of the data used in the focal mechanism determination (Figs. 3 and 4). Out of 67 polarities, 53 are consistent with the solution; as for the remaining 14, 10 originate from Westaway (1987) and other sources, and therefore cannot be verified. As mentioned above, our algorithm includes a test for the robustness of the solution based on the range of the values by which the three focal parameters can be changed without increasing the number of inconsistent polarities. Due to the fact that several stations happen to fall close to focal planes in the lower hemisphere focal projection (Fig. 4), this test has shown a range of variability of just ±1° for strike ϕ and of ±2–3° for dip δ and rake λ angles.

4. Discussion and conclusions

We characterized the source of the first shock of the 21 August 1962 (18:09 UTC) *Irpinia* sequence by obtaining well constrained parameters, such as its hypocentral location, magnitude, seismic moment, and focal mechanism (Fig. 4 and Table 5).

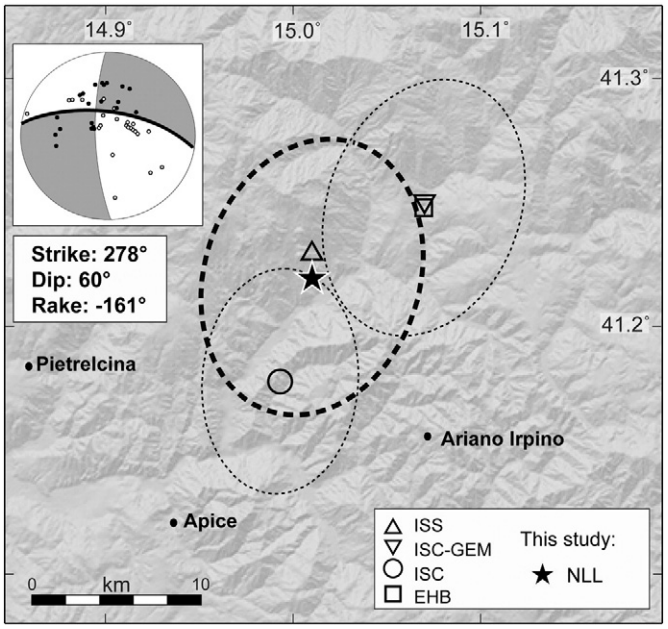

Fig. 4. Epicentral locations of the 21 August 1962, 18:09 earthquake from the literature and this study, with relevant error ellipses (if provided); focal mechanism from this study. We maintain that the north dipping, E-W striking, strike-slip fault plane is the most reliable plane.

We located this event with the NLL package obtaining the following hypocenter: 41.22°N, 15.01°E, and 9 km depth. Our epicenter is located between those by ISC (7 km to the SSW) and ISC-GEM and EHB (8 km to the NE), and is also in good agreement with the "old" ISS location. The error ellipse of our location partly overlaps those of ISC and ISC-GEM. Concerning the depth, we cannot compare our calculated value with the more recent results because they were fixed (see Table 1).

We computed magnitude and seismic moment (see Table 5) from the well recorded surface waves of our SISMOS seismograms scans. This raster dataset consists of low-gain analog and long-period electromagnetic regional seismograms recorded by high gain and high quality WWSSN seismographs (Fig. 3).

We calculated the focal mechanism for the 18:09 event from the first motion dataset read on the SISMOS seismograms integrated with those from Westaway (1987), and with 30 polarities from the ISC online bulletin, for a total of 67 polarities from 58 different stations (Table 4; Fig. 3). The reliability of our solution is supported by the very good azimuth and distance distribution of the data used to attain the focal mechanism. The test for the robustness of the solution has shown a limited range of variability of just ±1° for strike ϕ, and of ±2–3° for dip δ and rake λ. The focal mechanism exhibits strike-slip motion with a normal oblique component; nodal plane are north dipping, E-W striking, and west dipping, N-S striking, respectively (Fig. 4; Table 5).

The 21 August 1962 18:09, M_w 5.5, event occurred beneath the axial zone of the Apennine chain, and its causative fault roots at about 9 km. Given its location, the kinematics of this shock is currently considered rather unexpected. As a matter of fact, the strike-slip kinematics of the first event of the 1962 sequence significantly differs from that typically expected on the crest of the Apennines, characterized by almost purely

Table 5
Locations, magnitude, seismic moment, and focal mechanism of the 21 August 1962 18:09 UTC event from this study.

Lat (°)	Lon (°)	Depth (km)	M_w	Mo (dy ∗ cm) E24	Strike 1 (°)	Dip 1 (°)	Rake 1 (°)	Strike 2 (°)	Dip 2 (°)	Rake 2 (°)
41.22	15.01	9	5.5 ± 0.4	7.02	278	60	−161	178	73	−31

normal motion along NW-SE striking faults (e.g. 23 November 1980, M_w 6.9; Figs. 1 and 2).

The epicentre of the first event of the 21 August 1962 sequence is located near the earliest and southernmost source out of the three responsible for the destructive 1456 multiple earthquake (I_0 XI MCS; Fig. 2). The seismogenic source responsible for the southernmost 1456 event falls onto a ca. E-W tectonic trend, previously identified through macroseismic and geological analyses (Fracassi and Valensise, 2007), characterized by right-lateral motion (Basili et al., 2008; DISS Working Group, 2015).

The characteristics of the 21 August 1962, 18:09 source are nearly coincident with those of the E-W right-lateral strike-slip faults responsible for (a) the earliest earthquake of the 1456 sequence; (b) the 6 May 1971, M_w 5.0, *Monteleone* earthquake; (c) the 18 March 1992, M_w 4.1, earthquake; and (d) the 27 September 2012, M_w 4.6, *Benevento* earthquake (see Fig. 2).

Therefore, our preferred fault plane for the mechanism of the first event of the 21 August 1962 is the E-W striking one, as inferred from the geological features of the region, and from neighbouring seismogenic faults responsible for historical and instrumental events.

Our instrumental results confirm the existence in the Benevento area of an E-W striking, north dipping seismogenic fault system with right-lateral strike-slip kinematics. We do not know whether this fault system is also responsible for the other two main events of the 21 August 1962 sequence, since the parameters for the latter events are currently poorly constrained and in-depth studies are required. Hence, the locations and the geometric and kinematics parameters of the seismogenic sources responsible for the 1962 earthquakes are crucial to evaluate the extents and the continuity of the E-W shear zones beneath the Southern Apennines chain axial zone.

We conclude that (a) the first event of the 1962 sequence was generated by an individual segment of the regional E-W fault system; (b) the Sannio-Irpinia region is affected by a strike-slip fault system capable of destructive events like the main shocks of the 1962 and 1456 seismic sequences; and (c) strike-slip faulting participates in the tectonic deformation beneath the axial zone of the southern Apennines.

For the first time, instrumental data of a significant earthquake (M_w 5.5) shed light on strike-slip faulting beneath the Southern Apennines, suggesting that normal faulting is not the dominant tectonic style in this portion of the Italian peninsula. We maintain that the detailed study of the whole 1962 sequence will allow to explore the mechanisms of fault interaction in the southern Apennines between the extensional and transcurrent adjacent portions of the seismogenic layer.

Supplementary data to this article can be found online at http://dx.doi.org/10.1016/j.tecto.2016.10.032.

Acknowledgments

Comments of editor and reviewers helped improving the manuscript significantly. We are especially grateful to Umberto Fracassi for constructive comments and suggestions.

References

Adinolfi, G.M., De Matteis, R., Orefice, A., Festa, G., Zollo, A., de Nardis, R., Lavecchia, G., 2015. The September 27, 2012, M_L 4.1, Benevento earthquake: a case of strike-slip faulting in Southern Apennines (Italy). Tectonophysics 660:35–46. http://dx.doi.org/10.1016/j.tecto.2015.06.036.

Basili, A., Smriglio, G., Valensise, G., 1984. Procedure di determinazione ipocentrale in uso presso l'Istituto Nazionale di Geofisica. Atti Gruppo Nazionale di Geofisica della Terra Solida 875–884.

Basili, R., Valensise, G., Vannoli, P., Burrato, P., Fracassi, U., Mariano, S., Tiberti, M.M., Boschi, E., 2008. The Database of Individual Seismogenic Sources (DISS), version 3: summarizing 20 years of research on Italy's earthquake geology. Tectonophysics 453:20–43. http://dx.doi.org/10.1016/j.tecto.2007.04.014.

Bernardi, F., Braunmiller, J., Giardini, D., 2005. Seismic moment from regional surface-wave amplitudes: applications to digital and analog seismograms. B. Seismol. Soc. Am. 95:408–418. http://dx.doi.org/10.1785/0120040048.

Bernardi, F., Ciaccio, M.G., Palombo, B., Ferrari, G., 2016. Moment tensor inversion of early instrumental data: application to the 1917 High Tiber Valley, Monterchi earthquake. Ann. Geoph. 59 (S0318):1–13. http://dx.doi.org/10.4401/ag-6850.

Bigi, G., et al., 1989. Synthetic structural-kinematic map of Italy. In: Structural Model of Italy. C.N.R. Progetto Finalizzato Geodinamica scale 1:500,000. (Quaderni della Ricerca Scientifica 114).

Bonasia, V., Cagnetti, V., De Natale, G., Pingue, F., Scarpa, R., 1986. Studio dei Processi Sismotettonici nell'Appennino Centro-Meridionale dall'interpretazione dei dati sismici e di Deformazione del Suolo. Atti GNGTS, 5° Conv., Roma, pp. 539–566.

Byerly, P., 1928. The nature of the first motion in the Chilean earthquake of November 11, 1922. Am. J. Sci. 1 (6), 232–236 Series 5.

Byerly, P., 1942. Seismology. Prentice-Hall, New York, pp. 221–242.

Carrozzo, M.T., De Visintini, G., Giorgetti, F., Iaccarino, E., 1973. General Catalogue of Italian Earthquakes. CNEN, RT/PROT 73, 12, Roma (225 pp).

Charlier, C., Van Gils, J.M., 1953. Liste des stations séismologiques mondiales (282 pp).

Constantinescu, L., Ruprechtovß, L., Enescu, D., 1966. Mediterranean-alpine earthquake mechanisms and their seismotectonic implications. Geophys. J. R. Astr. Soc. 10, 347–368.

De Bremaecker, J.C., 1956. Remark on Byerly's fault-plane method. Bull. Seism. Soc. Am. 46 (3), 215–216.

Di Filippo, D., Peronaci, F., 1963. Indagine preliminare della natura fisica del fenomeno che ha originato il periodo sismico irpino dell'Agosto 1962. Ann. Geofis. 16, 625–643.

DISS Working Group, 2015. Database of Individual Seismogenic Sources (DISS), Version 3.2.0: A Compilation of Potential Sources For Earthquakes Larger Than M 5.5 in Italy and Surrounding Areas. http://diss.rm.ingv.it/diss/. Istituto Nazionale di Geofisica e Vulcanologia http://dx.doi.org/10.6092/INGV. IT-DISS3.2.0.

Doglioni, C., Harabaglia, P., Martinelli, G., Mongelli, F., Zito, G., 1996. A geodynamic model of the Southern Apennines accretionary prism. Terra Nova 8, 540–547.

Ferrari, G., Pino, N.A., 2003. EUROSEISMOS 2002-2003 a project for saving and studying historical seismograms in the Euro-Mediterranean area. Geophys. Res. Abstr. 5, 05274.

Fracassi, U., Valensise, G., 2007. Unveiling the sources of the catastrophic 1456 multiple earthquake: hints to an unexplored tectonic mechanism in southern Italy. B. Seismol. Soc. Am. 97 (3), 725–748.

Frepoli, A., Amato, A., 2000. Fault plane solutions of crustal earthquakes in southern Italy (1988–1995): seismotectonic implications. Ann. Geofis. 43 (3), 437–467.

Frohlich, C., 1992. Triangle diagrams: ternary graphs to display similarity and diversity of earthquake focal mechanisms. Physics of the Earth and Planetary Interior 75, 193–198.

Galitzin, F.B., 1914. Vorlesungen über Seismometrie. B.G. Teuner, Berlin, Germany.

Gasparini, C., Iannaccone, G., Scandone, P., Scarpa, R., 1982. Seismotectonics of Calabrian Arc. Tectonophysics 84, 267–286.

Gasparini, C., Iannaccone, G., Scarpa, R., 1985. Fault-plane solutions and seismicity of the Italian peninsula. Tectonophysics 117, 59–78.

Gasperini, P., Bernardini, F., Valensise, G., Boschi, E., 1999. Defining seismogenic sources from historical earthquake felt reports. Bull. Seismol. Soc. Am. 89, 94–110.

Gasperini, P., Vannucci, G., Tripone, D., Boschi, E., 2010. The location and sizing of historical earthquakes using the attenuation of macroseismic intensity with distance. Bull. Seismol. Soc. Am. 100 (5A):2035–2066. http://dx.doi.org/10.1785/0120090330.

Gasperini, P., Lolli, B., Vannucci, G., 2013. Empirical calibration of local magnitude data sets versus moment magnitude in Italy. Bull. Seismol. Soc. Am. 103 (4):2227–2246. http://dx.doi.org/10.1785/0120120356.

Gruppo di Lavoro ZS9, 2004. Redazione della mappa della pericolosità sismica prevista dall'Ordinanza PCM 3274 del 20 marzo 2003. Rapporto Conclusivo per il Dipartimento della Protezione Civile, INGV, Milano-Roma aprile 2004. 65 pp + 5 appendici. (website) http://zonesismiche.mi.ingv.it/.

Guidoboni, E., Ferrari, G., Mariotti, D., Comastri, A., Tarabusi, G., Valensise, G., 2007. CFTI4Med, Catalogue of Strong Earthquakes in Italy (461 B.C.-1997) and Mediterranean Area (760 B.C.-1500). INGV-SGA. http://storing.ingv.it/cfti4med/.

Gutenberg, B., 1945. Amplitudes of Rayleigh-waves and magnitude of shallow earthquakes. Bull. Seism. Soc. Am. 35, 3–12.

Hagiwara, T., 1958. A note on the theory of the electromagnetic seismograph. Bull. Earth. Res. Inst. 36, 139–164.

Hanks, T.C., Kanamori, H., 1979. A moment magnitude scale. J. Geophys. Res. 84, 2348–2350.

International Seismological Centre (ISC). (December) 2015 On-line Bulletin, http://www.isc.ac.uk/iscbulletin/search/bulletin/, Internatl. Seis. Cent., Thatcham, United Kingdom.(Last accessed).

ISIDe Working Group, 2016. Italian seismological instrumental and parametric database. http://iside.rm.ingv.it.

ISS, 1967. Bulletin of the International Seismological Summary for 1962. http://storing.ingv.it/ISS/JPG/i62q3ind.html.

Kárník, V., Kondorskaya, N., Riznitchenko, J., Savarensky, E., Soloviev, S., Shebalin, N., Vaněk, N., Zátopek, A., 1962. Standardisation of the earthquake magnitude scale. Stud. Geophys. Geod. 6, 42–47.

Kennett, B.L.N., 2005. Seismological Tables: ak135, Research School of Earth Sciences. The Australian National University, Canberra, Australia (290 pp).

Kiratzi, A.A., Papazachos, C.B., 1995. Active crustal deformation from the Azores triple junction to the Middle East. Tectonophysics 243, 1–24.

Kostrov, V.V., 1974. Seismic moment and energy of earthquakes and seismic flow of rock. Izv. Acad. Sci. USSR Phys. Solid Earth 1, 13–21.

Li, H., Michelini, A., Zhu, L., Bernardi, F., Spada, M., 2007. Crustal velocity structure in Italy from analysis of regional seismic waveforms. Bull. Seism. Soc. Am. 97 (6):2024–2039. http://dx.doi.org/10.1785/0120070071.

Locati, M., Camassi, R., Stucchi, M. (Eds.), 2011. DBMI11, la versione 2011 del Database Macrosismico Italiano (Milano, Bologna), http://emidius.mi.ingv.it/DBMI11, doi: 10.6092/INGV.IT-DBMI11.

Lomax, A., 2005. A reanalysis of the hypocentral location and related observations for the great 1906 California earthquake. Bull. Seismol. Soc. Am. 95:861–877. http://dx.doi.org/10.1785/0120040141.

Malinverno, A., Ryan, W.B.F., 1986. Extension in the Tyrrhenian Sea and shortening in the Apennines as result of arc migration driven by sinking of the lithosphere. Tectonics 5, 227–245.

Michelini, A., De Simoni, B., Amato, A., Boschi, E., 2005. Collecting, digitizing, and distributing historical seismological data. Eos Trans. AGU 86 (28):261–266. http://dx.doi.org/10.1029/2005EO280002.

Michetti, A.M., Brunamonte, F., Serva, L., Vittori, E., 1996. Trench investigations of the 1915 Fucino earthquake fault scarp (Abruzzo, central Italy): geological evidence of large historical events. J. Geophys. Res. 101 (B3), 5921–5936.

Milano, G., Di Giovambattista, R., Ventura, G., 2006. Seismicity and stress field in the Sannio-Matese area. Ann. Geophys. Supplement to vol. 49 (1).

Peterson, J., Hutt, C.R., 2014. World-Wide Standardized Seismograph Network-A data users guide: U.S. Geological Survey Open-File Report 2014–1218. 74pp. http://dx.doi.org/10.3133/ofr20141218.

Pino, N.A., Palombo, B., Ventura, G., Perniola, B., Ferrari, G., 2008. Waveform modeling of historical seismograms of the 1930 Irpinia earthquake provides insight on "blind" faulting in Southern Apennines (Italy). J. Geophys. Res. 113 (B05303). http://dx.doi.org/10.1029/2007JB005211.

Rovida, A., Camassi, R., Gasperini, P., Stucchi, M. (Eds.), 2011. CPTI11, the 2011 version of the Parametric Catalogue of Italian Earthquakes (Milano, Bologna), http://emidius.mi.ingv.it/CPTI, doi: 10.6092/INGV.IT-CPTI11.

Shishkevish, C., 1974. Soviet Seismographic stations and seismic instruments. Part I, Report R-1204-ARPA. Rand Corporation (200 pp).

Soloviev, S.L., 1955. O klassifikatsii zemletrasenii po velichine ikh energii, Trudi Geofiz. Inst. Akad. Nauk SSSR 30, 3–31.

Storchak, D.A., Di Giacomo, D., Bondár, I., Engdahl, E.R., Harris, J., Lee, W.H.K., Villaseñor, A., Bormann, P., 2013. Public release of the ISC-GEM global instrumental earthquake catalogue (1900–2009). Seism. Res. Lett. 84 (5):810–815. http://dx.doi.org/10.1785/0220130034.

Vaněk, N., Kârnik, V., Zâtopek, A., Kondorskaya, N., Riznitchenko, J., Savarensky, E.F., Soloviev, S.V., Shebalin, N., 1962. Standardisation of magnitude scales. Bull. Acad. Sci. USSR Geophys. Ser. 2, 108–111.

Vannoli, P., Burrato, P., Valensise, G., 2015a. The seismotectonic of the Po Plain (northern Italy): tectonic diversity in a blind faulting domain. Pure Appl. Geophys. 172 (5): 1105–1142. http://dx.doi.org/10.1007/s00024-014-0873-0.

Vannoli, P., Vannucci, G., Bernardi, F., Palombo, F., Ferrari, G., 2015b. The source of the 30 October 1930, Mw 5.8, Senigallia (central Italy) earthquake: a convergent solution from instrumental, macroseismic and geological data. B. Seismol. Soc. Am. 105 (3): 1548–1561. http://dx.doi.org/10.1785/0120140263.

Vannucci, G., Gasperini, P., 2004. The new release of the database of earthquake mechanisms of the Mediterranean area (EMMA version 2). Ann. Geophys. 47, 303–327 Supplement to.

Villaseñor, A., Engdahl, E.R., 2005. A digital hypocenter catalog for the International Seismological Summary (ISS). Seismol. Res. Lett. 76, 554–559.

Westaway, R., 1987. The Campania, Southern Italy, earthquakes of 1962 August 21. Geophys. J. R. Astr. Soc. 88, 1–24.

Westaway, R., Jackson, J., 1984. Surface faulting in the southern Italian Campania-Basilicata earthquake of 23 November 1980. Nature 312, 436–438.

Willmore, P.L., 1979. Manual of Seismological Observatory Practice. World Data Center A for Solid Earth Geophysics, Boulder, Colorado.